

# Stringent constraints on cosmological neutrino-antineutrino asymmetries from synchronized flavor transformation

Kevork N. Abazajian, John F. Beacom, and Nicole F. Bell

*NASA/Fermilab Astrophysics Center, Fermi National Accelerator Laboratory, Batavia, Illinois 60510-0500*

[aba@fnal.gov](mailto:aba@fnal.gov), [beacom@fnal.gov](mailto:beacom@fnal.gov), [nfb@fnal.gov](mailto:nfb@fnal.gov)

(Dated: March 25th, 2002)

We assess a mechanism which can transform neutrino-antineutrino asymmetries between flavors in the early universe, and confirm that such transformation is unavoidable in the near bi-maximal framework emerging for the neutrino mixing matrix. We show that the process is a standard Mikheyev-Smirnov-Wolfenstein flavor transformation dictated by a synchronization of momentum states. We also show that flavor “equilibration” is a special feature of maximal mixing, and carefully examine new constraints placed on neutrino asymmetries. In particular, the big bang nucleosynthesis limit on electron neutrino degeneracy  $|\xi_e| \lesssim 0.04$  does not apply directly to all flavors, yet confirmation of the large-mixing-angle solution to the solar neutrino problem will eliminate the possibility of degenerate big bang nucleosynthesis.

PACS numbers: 14.60.Pq, 26.35.+c

FERMILAB-Pub-02/056-A

## I. INTRODUCTION

As is well known, the observational successes of big bang nucleosynthesis (BBN) are one of the pillars of standard cosmology [1]. If one assumes three standard neutrino flavors, then the only free parameter is the baryon to photon ratio  $n_B/n_\gamma$ . The value  $n_B/n_\gamma \simeq 5 \times 10^{-10}$  predicts light-element yields of  $^2\text{H}$ ,  $^4\text{He}$ , and  $^7\text{Li}$  that are in excellent agreement with observations. As is often noted, this is particularly remarkable because the absolute yields of these elements span several orders of magnitude. This consistency implies that the post-BBN processing of the light elements is largely understood, and that one does not require new aspects of particle physics beyond the standard model (SM) that would materially affect BBN.

The basic consistency of our picture of the early universe is even more impressive when one considers other recent cosmological measurements. Observations of the acoustic peaks in the angular power spectrum of the cosmic microwave background (CMB) give strong evidence that  $\Omega_{total} = 1.04 \pm 0.06$  [2], i.e., the universe is flat, as predicted by inflation. Taken together with measurements of clusters of galaxies and the high-redshift type-Ia supernovae (SNIa) data, a mutually consistent picture [3] with  $\Omega_{matter} \simeq 0.3$  and  $\Omega_{lambda} \simeq 0.7$  is obtained. Additionally, the CMB data indicate that  $\Omega_{baryon} \simeq 0.04$ , in excellent agreement with the BBN observations. Recent data on the clustering of galaxies also yield consistent values of  $\Omega_{matter}$  and  $\Omega_{baryon}$  [4]. This agreement of the combined data is all the more impressive because baryonic matter is such a small fraction of the total energy density of the universe, and because the BBN and CMB data reflect measurements of  $\Omega_{baryon}$  at very different epochs ( $\sim 10^2$  s and  $\sim 10^{13}$  s after the big bang, respectively).

Nevertheless, from a particle-physics point of view, these impressively measured quantities are all totally unexplained, both in their values and their nature (e.g.,

though we know that the particle dark matter is not part of the SM, we do not know what it is). Just as in accelerator-based particle physics, the underlying belief is that more and more precise measurements will lead us to the necessary clues on how to generalize the SM. In particular, the baryon-antibaryon asymmetry of  $5 \times 10^{-10}$  remains a mystery, and is certainly an important clue for understanding the universe at temperatures at least as high as the electroweak scale.

Naturally, attention is also focused on the lepton-antilepton asymmetry of the universe. General considerations indicate that  $B - L$  may be conserved, so that the lepton asymmetry is  $n_L/n_\gamma \simeq 5 \times 10^{-10}$  as well. However, there are certainly viable models in which the lepton asymmetry can be much larger [5], and if confirmed, would be a very important clue. Given constraints on charge asymmetry, any large lepton asymmetry would have to be hidden in the neutrino sector. Though the baryon asymmetry can generically be limited to be less than  $10^{-8}$  simply to not overclose the universe, no similar constraints exist in the lepton sector for light neutrinos.

Since neutrinos and antineutrinos should be in chemical equilibrium until they decouple at a temperature  $T \sim 2$  MeV, they may be well described by Fermi-Dirac distributions with equal and opposite chemical potentials:

$$f(p, \xi) = \frac{1}{1 + \exp(p/T - \xi)}, \quad (1.1)$$

where  $p$  denotes the neutrino momentum,  $T$  the temperature and  $\xi$  is the chemical potential in units of  $T$ . (There is a tiny non-thermal perturbation that occurs at the epoch of  $e^+e^-$  annihilation at  $T \simeq 0.3$  MeV, which we can ignore.) The lepton asymmetry  $L_\alpha$  for a given flavor  $\nu_\alpha$  is related to the chemical potential by

$$L_\alpha = \frac{n_{\nu_\alpha} - n_{\bar{\nu}_\alpha}}{n_\gamma} = \frac{\pi^2}{12\zeta(3)} \left( \xi_\alpha + \frac{\xi_\alpha^3}{\pi^2} \right), \quad (1.2)$$

where  $\zeta(3) \simeq 1.202$ . Even enormous values of  $\xi_\alpha \sim 1$  have been allowed observationally. This is so distant from the naive SM prediction that any measured nonzero value would be very important. Interest in searches for such large values of  $\xi_\alpha$  is also driven by the fact that we evidently have much to learn about the neutrino sector. Previously, most attention was devoted to the possibility of significant mixing of the SM active neutrinos with light sterile neutrinos, which can generate large lepton numbers  $L \sim 1$  [6].

A general approach to setting limits on  $\xi_\alpha$  arises because for very large degeneracy, the effective number of neutrinos is increased from the standard model prediction by

$$\Delta N_\nu = \frac{30}{7} \left( \frac{\xi}{\pi} \right)^2 + \frac{15}{7} \left( \frac{\xi}{\pi} \right)^4. \quad (1.3)$$

This increases the expansion rate of the universe, changing the CMB results by magnifying the amplitude of the acoustic peaks. For all flavors, the bound  $|\xi_\alpha| \lesssim 3$  has been obtained from the CMB alone [7]. Note that the sign of  $\xi_\alpha$  is unconstrained. With future CMB data, these limits may be reduced to  $|\xi_\alpha| \lesssim 0.25$  or less [8]. A much stronger limit can be placed on  $\xi_e$  with  $|\xi_e| \lesssim 0.04$  because of its effect on setting the neutron to proton ratio prior to BBN by altering beta equilibrium.<sup>1</sup> If at the same time  $\xi_{\mu,\tau}$  are large, this effect can be partially undone by the increased expansion rate, leading to the often-quoted bounds [9, 10]

$$-0.01 < \xi_e < 0.22, \quad (1.4)$$

$$|\xi_{\mu,\tau}| < 2.6, \quad (1.5)$$

where the upper limits are obtained only in tandem.

There are now three types of evidence for neutrino oscillations: solar neutrino [11]  $\nu_e \rightarrow \nu_\mu, \nu_\tau$  with large (but not maximal) mixing angle and  $\delta m^2 \simeq 10^{-5} \text{ eV}^2$ , atmospheric [12] neutrino  $\nu_\mu, \bar{\nu}_\mu \rightarrow \nu_\tau, \bar{\nu}_\tau$  with maximal mixing and  $\delta m^2 \simeq 10^{-3} \text{ eV}^2$ , and the Liquid Scintillator Neutrino Detector (LSND) [13] neutrino  $\bar{\nu}_\mu \rightarrow \bar{\nu}_e$  with a very small angle and  $\delta m^2 \simeq 1 \text{ eV}^2$ . It is not possible to accomodate these three signals with only three neutrinos, as there are only two independent mass-squared differences. A possible fourth (sterile) neutrino can be invoked to create a new  $\delta m^2$ , but now that the solar and atmospheric neutrino data indicate the appearance of active neutrino flavors, there is a problem of where to incorporate the required mixing with the sterile neutrino. While four-neutrino models may still work, it is only with difficulty, both in fitting the oscillation data (see, e.g., Ref. [14]) and through the effects on BBN (see, e.g., Ref. [15]). The LSND signal will be conclusively

confirmed or refuted by the MiniBooNE experiment [16]. For simplicity, we consider just three active neutrinos, and neglect the LSND result (of course, if it is confirmed, a major revision will be necessary).

In such a three-neutrino framework, Lunardini and Smirnov [17] suggested that the large mixing angles implied by the present data may transfer any large asymmetry hidden in  $\xi_{\mu,\tau}$  to  $\xi_e$  well before the beta-equilibrium freezeout at  $T \simeq 1 \text{ MeV}$  (see also Savage, Malaney and Fuller [18]). Thus, the stringent BBN limit on  $\xi_e$  might apply to all three flavors, improving the bounds on  $\xi_{\mu,\tau}$  by nearly two orders of magnitude.

This proposal was recently studied in detail by Dolgov, Hansen, Pastor, Petcov, Raffelt, and Semikoz (DHPPRS) [19]. They found that close to complete transformation of asymmetries  $\xi_\mu$  and  $\xi_\tau$  to  $\xi_e$  was obtained. This is an important result, as it excludes the possibility of degenerate BBN [20], and is the strongest limit on the total lepton number of the universe and is likely to remain so for the foreseeable future. In this article we examine the DHPPRS result, show it as the result of a synchronized Mikheyev-Smirnov-Wolfenstein (MSW) transformation and establish its robustness through physical and numerical insight into the dynamics. We assess how the results depend on the input parameters and consider more exotic physical scenarios that might affect the results.

## II. TWO-FLAVOR DENSITY MATRIX EQUATIONS AND SYNCHRONIZED MSW

In this section we consider a mixed neutrino statistical ensemble in the early universe, with initial neutrino-antineutrino asymmetries which are not equal among flavors. We show that this ensemble behaves as a synchronized system following a single effective momentum state that undergoes an MSW transformation given large mixing angles. In describing neutrino flavor evolution in dense environments such as the early universe, one must use a density matrix description if the neutrino self-potential is large or if decohering collisional processes are significant. Where collisional processes are not important, as is the case for some examples we shall consider here, the evolution is coherent. A useful parametrization of the density matrix equations is the Bloch form [21].

In an environment such as the early universe, where the potential arising from neutrino-neutrino forward scattering (the neutrino self-potential) is important, active-active mixing is substantially different from active-sterile mixing. Forward scattering processes of the type  $\nu_\alpha(p) \rightarrow \nu_\beta(p)$  lead to refractive index terms which are off-diagonal in the flavor basis  $\{\alpha, \beta\}$  [22]. A useful and interesting casting of the Bloch formalism for pure active neutrino mixing was done by Pastor, Raffelt and Semikoz [23], which allows an interpretation via analogy with the precession of coupled magnetic dipoles. The analysis of Ref. [23] considered the case of constant density, in the

---

<sup>1</sup> Beta equilibrium is between the weak interactions  $n + \nu_e \leftrightarrow p + e^-$  and  $p + \bar{\nu}_e \leftrightarrow n + e^+$ . Positive  $\xi_e$  increases the  $\nu_e$  abundance relative to  $\bar{\nu}_e$ , forcing equilibrium towards lower  $n/p$ .

absence of a background medium other than that provided by the neutrinos themselves. We shall have need to extend this description to include a background medium of charged leptons of a density that varies with time (or temperature). One particularly interesting feature first revealed clearly in Ref. [23], is that the neutrino self-potential (that is, the potential due to neutrino-neutrino forward scattering) does not, in general, suppress flavor oscillations, as one might have naively expected by analogy with the potential from, say, a background of charged leptons. This is in stark contrast to the case of active-sterile oscillations, where the effect of an asymmetry between the active neutrinos and antineutrinos is always to suppress mixing angles. Even for relatively small degeneracies, the asymmetry term dominates the evolution and thus delays transformation of such asymmetry from the active to the sterile flavor.

For active-active oscillations, no such simple mixing angle suppression occurs as the neutrino asymmetry enters both the diagonal and off-diagonal terms in the effective Hamiltonian. These terms have the effect of synchronizing the ensemble,<sup>2</sup> resulting in collective behavior resembling the evolution of a single momentum state in the absence of the self-potential. The mixing angle for this collective oscillation is determined essentially by the background medium of thermal charged leptons. When the density of this background decreases with temperature, the neutrinos evolve adiabatically from their initial flavor into vacuum mass eigenstates. For large-angle mixing, this implies significant flavor transformation.

### A. Formulation

We express the mixing between two neutrino mass and flavor eigenstates as

$$\begin{aligned}\nu_e &= \cos \theta_0 \nu_1 + \sin \theta_0 \nu_2, \\ \nu_\mu^* &= -\sin \theta_0 \nu_1 + \cos \theta_0 \nu_2,\end{aligned}\quad (2.1)$$

where, in general,  $\nu_\mu^*$  denotes some linear superposition of  $\nu_\mu$  and  $\nu_\tau$ , as we shall explain later. We parametrize the two-flavor neutrino density matrix in the form

$$\rho(p) = \begin{pmatrix} \rho_{ee} & \rho_{e\mu} \\ \rho_{\mu e} & \rho_{\mu\mu} \end{pmatrix} = \frac{1}{2} [P_0(p) + \boldsymbol{\sigma} \cdot \mathbf{P}(p)], \quad (2.2)$$

and similarly for the antineutrinos, where we refer to  $\mathbf{P}(p)$  as the neutrino “polarization” vector. These quantities are most usefully normalized such that

$$\mathbf{P}(p)^{initial} = \frac{1}{n^{eq}/T^3} [f_e(p, \xi_e) - f_\mu(p, \xi_\mu)], \quad (2.3)$$

---

<sup>2</sup> Note that this forward-scattering induced synchronization is unrelated to the synchronization effect of Ref. [24] which arises from rapid flavor-blind collisions. It is remarkable that both collisions and forward scattering lead to synchronization effects in the case of active-active oscillations.

where  $n_0^{eq} = \int d^3 p / (2\pi)^3 f(p, 0) = 3\zeta(3)T^3/4\pi^2$ .

In the absence of collision terms,  $P_0(p)$  and the magnitude of  $\mathbf{P}(p)$  remain constant and the full evolution equations for two mixed active flavors in the early universe are

$$\begin{aligned}\partial_t \mathbf{P}_p &= +\mathbf{A}_p \times \mathbf{P}_p + \alpha(\mathbf{J} - \bar{\mathbf{J}}) \times \mathbf{P}_p, \\ \partial_t \bar{\mathbf{P}}_p &= -\bar{\mathbf{A}}_p \times \bar{\mathbf{P}}_p + \alpha(\mathbf{J} - \bar{\mathbf{J}}) \times \bar{\mathbf{P}}_p,\end{aligned}\quad (2.4)$$

where  $\mathbf{P}_p$  denotes the polarization vectors for the neutrinos of momentum  $p$  while  $\mathbf{J}$  denotes the corresponding quantity integrated over momentum such that

$$\mathbf{J} = \int \frac{d^3(p/T)}{(2\pi)^3} \mathbf{P}_p. \quad (2.5)$$

Vectors with an overbar refer to the antineutrino quantities throughout. With the normalization we use here, the length of the individual  $\mathbf{P}_p$  vectors and that of  $\mathbf{J}$  do not redshift with temperature. The coefficient of the second term is  $\alpha \equiv \sqrt{2}G_F n^{eq}$ . Time  $t$  and temperature  $T$  may be interconverted via the expression  $t \simeq 1.15 \text{ s} (T/\text{MeV})^{-2}$ . Decohering collisions (damping) of the system at high temperatures forces the neutrinos into unmixed flavor states. We shall assume zero initial  $\xi_e^i$  and a finite initial  $\xi_\mu^i$ , taken to have a negative sign.<sup>3</sup> Therefore, the initial alignment of the  $\mathbf{P}_p$  are along the  $+z$  axis, and  $\bar{\mathbf{P}}_p$  are along the  $-z$  axis.

Equations (2.4) are equivalent to the precession of magnetic dipoles in two “magnetic fields”: the momentum-dependent  $\mathbf{A}_p$  and the integrated neutrino self-potential  $\alpha(\mathbf{J} - \bar{\mathbf{J}})$ . The effects of  $\mathbf{A}_p$ , as we shall show, are straightforward, but the neutrino self-potential makes the system non-linear by explicitly coupling each momentum mode to the evolution of every other momentum mode. An intuitive description of the evolution in Eq. (2.4) for a constant-density system without matter effects was provided in Ref. [23]. The issue of the synchronization of the system has also been studied in Ref. [25].

In general, the “magnetic field” vector  $\mathbf{A}_p$  includes contributions from vacuum mixing, a thermal potential from the charged-lepton background, and a potential due to asymmetries between the charged leptons

$$\mathbf{A}_p = \Delta_p + [V^T(p) + V^B] \hat{\mathbf{z}}. \quad (2.6)$$

Vacuum mixing is incorporated by

$$\Delta_p = \frac{\delta m_0^2}{2p} (\sin 2\theta_0 \hat{\mathbf{x}} - \cos 2\theta_0 \hat{\mathbf{z}}), \quad (2.7)$$

where  $\delta m_0^2 = m_2^2 - m_1^2$  and  $\theta_0$  are the vacuum oscillation parameters.

---

<sup>3</sup> For the opposite sign, one simply reverses the directions of the polarization vectors.

The thermal potential from finite-temperature modification of the neutrino mass due to the presence of thermally populated charged leptons in the plasma is

$$V^T(p) = -\frac{8\sqrt{2}G_F p}{3m_W^2} (\langle E_{l^-} \rangle n_{l^-} + \langle E_{l^+} \rangle n_{l^+}). \quad (2.8)$$

The neutrinos also contribute a *thermal* self-potential similar to the form of the self-potential on the right-hand side (RHS) of Eqs. (2.4) [26], but unlike  $\alpha \sim G_F$ , the thermal self-potential goes as  $G_F^2$ . Unless the initial asymmetry is of a size much too small to be interesting here, the  $G_F^2$  term is negligible by comparison with the order  $G_F$  self-potential and thus unimportant in determining the dynamics of the system.

The background potential arising due to asymmetries in charged leptons is nonzero only for electron neutrinos to maintain charge neutrality of the baryon-contaminated plasma:

$$V^B = \begin{cases} \pm\sqrt{2}G_F(n_{e^-} - n_{e^+}) & \text{for } \nu_e = \nu_{\mu,\tau}, \\ 0 & \text{for } \nu_\mu = \nu_\tau, \end{cases} \quad (2.9)$$

where  $+(-)$  is for neutrinos (antineutrinos). Due to the smallness of the baryon asymmetry relative to number densities of thermalized species, this term is always negligibly small relative to the vacuum vector  $\Delta_p$  and the thermal potential  $V^T$ , and so we may take  $\overline{\mathbf{A}}_p = \mathbf{A}_p$ .

In the absence of the neutrino self-potential it is possible to define

$$\mathbf{A}_p \equiv \frac{\delta m_m^2}{2p} (\sin 2\theta_m \hat{\mathbf{x}} - \cos 2\theta_m \hat{\mathbf{z}}), \quad (2.10)$$

where  $\delta m_m^2$  and  $\theta_m$  are the matter-affected oscillation parameters. When the self-term must be included, the nonlinearity of the problem makes the notion of a matter-affected mixing angle more subtle.

## B. Synchronization

Taking the difference of the Eqs. (2.4), integrating over momenta, and defining a collective polarization vector  $\mathbf{I} \equiv \mathbf{J} - \overline{\mathbf{J}}$  one obtains

$$\partial_t \mathbf{I} \simeq \mathbf{A}_{\text{eff}} \times \mathbf{I}, \quad (2.11)$$

where the appropriate effective “magnetic field” is

$$\mathbf{A}_{\text{eff}} \simeq \frac{1}{\mathbf{I}^2} \int \mathbf{A}_p (\mathbf{P}_p + \overline{\mathbf{P}}_p) \cdot \mathbf{I}. \quad (2.12)$$

In fact, Eqs. (2.11), (2.12) are exact only when  $\mathbf{I} \parallel (\mathbf{P}_p + \overline{\mathbf{P}}_p)$ . The vector  $\mathbf{I}$  thus precesses slowly about  $\mathbf{A}_{\text{eff}}$ . Since the self-potential dominates Eqs. (2.4), the individual polarization vectors  $\mathbf{P}_p$  all precess rapidly about  $\mathbf{I}$ , and, if initially aligned, are held together. The various vectors are illustrated in Fig. 1.

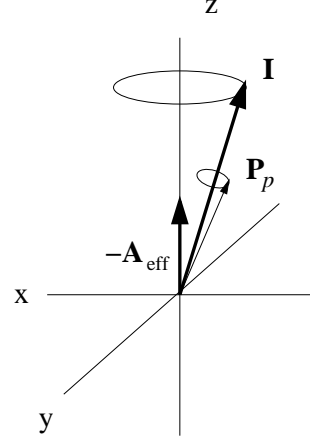


FIG. 1: Vector precession diagram. The angles and magnitudes of the vectors are not to scale but have been exaggerated for clarity. For the situation of interest, the magnitude of  $\mathbf{I}$  is much greater than that of  $\mathbf{A}_{\text{eff}}$ . When this condition holds, it is a good approximation to describe the evolution of the polarization vectors for the individual momentum modes  $\mathbf{P}_p$  as a precessing about  $\mathbf{I}$ . The vector  $\mathbf{I}$  then precesses about  $\mathbf{A}_{\text{eff}}$ , in the manner of a single momentum mode in the absence of the self-term. For asymmetries between neutrino flavors in the early universe,  $\mathbf{A}_{\text{eff}}$  and  $\mathbf{I}$  are both initially aligned with the  $z$  axis, and, for maximal mixing, both adiabatically evolve to align with the  $x$  axis.

We assume for simplicity that the initial asymmetry resides in a single flavor. Although the coefficient of the self-term makes it dominant, the flavor transformation is actually determined by the evolution of  $\mathbf{A}_{\text{eff}}$ . In fact, if one leaves out the self-term altogether, the synchronization is of course lost, but the average flavor evolution of the system is almost completely unchanged.

Let us first consider the simple linearized case where the self-potentials in Eqs. (2.4) vanish. In this case, the polarization vector of each momentum mode  $\mathbf{P}_p$  precesses about its own respective  $\mathbf{A}_p$ :

$$\begin{aligned} \partial_t \mathbf{P}_p &= +\mathbf{A}_p \times \mathbf{P}_p, \\ \partial_t \overline{\mathbf{P}}_p &= -\mathbf{A}_p \times \overline{\mathbf{P}}_p. \end{aligned} \quad (2.13)$$

If one follows only the average momentum  $\langle p/T \rangle \simeq 3.15$ , Eqs. (2.13) are simply two linear equations with a straightforward solution. Recall that each  $\mathbf{P}_p$  is initially aligned along the  $+z$  axis. At high temperatures,  $|V^T| \gg |\Delta_p|$ , and thus from Eq. (2.6) the  $\mathbf{A}_p$  point in the  $-\hat{\mathbf{z}}$  direction. As the temperature of the universe decreases,  $|V^T| \sim T^5$  decreases and the vectors  $\mathbf{A}_p$  will slowly rotate from the  $-\hat{\mathbf{z}}$  direction toward the  $+\hat{\mathbf{x}}$  direction and the angle that  $\mathbf{A}_p$  subtends with the  $z$  axis will asymptote to  $2\theta_0$ . This effect is a straightforward MSW transformation of the asymmetry: the initial neutrino number excess in one flavor evolves from a mass eigenstate in matter (modified by the thermal potential) to a vacuum mass eigenstate with different flavor content. And, since Eqs. (2.13) are decoupled, the average-

momentum mode will describe the collective evolution of the entire system.

In the substantially more involved system, including the self-potential (2.4), each momentum mode is coupled to all other momenta through the self-term. Therefore, a simplifying average-momentum technique is poorly justified. However, if one blindly drives forward with an average-momentum evolution of Eqs. (2.4), one luckily recovers (nearly) the correct behavior. For the full-momentum case, including the self-potential, the  $\mathbf{I}$  vector will also initially be aligned with the  $z$  axis. Using the approximate Eqs. (2.11) and making the as-yet unjustified assumption that  $\mathbf{A}_{\text{eff}}$  follows the *average* of the  $\mathbf{A}_p$ , the synchronized system will undergo the MSW transformation at the exact same temperature as the over simplified case (2.13). This is what we found numerically.

The fact that the neutrino flavor system evolves to the same end-state with and without the self-term appears at first absurd. However, one must keep in mind that the neutrino self-potential in a purely active neutrino system affects the evolution drastically differently than the familiar flavor-diagonal potentials in the matter Hamiltonian present, for example, in evaluating the solar MSW effect and active-sterile mixing in the early universe. The neutrino self-potential, as the dominant precession term for each momentum, only plays the role of forcing each momentum mode to follow the collective vector  $\mathbf{I}$ .

To explore the behavior of the system and verify the approximations in arriving at the collective equations (2.11), (2.12), we numerically integrate Eqs. (2.4), which, again, explicitly couple the full thermal distribution of momenta to the quantum mechanical evolution of each momentum mode. Because of the drastically different time scales over which the terms  $\Delta_p$ ,  $V^T(p)$  and  $\alpha(\mathbf{J} - \bar{\mathbf{J}})$  evolve, the system is a set of stiff nonlinear differential equations and therefore requires careful treatment.

In Fig. 2a we show the evolution with the full equations (2.4) of a representative two-flavor  $\nu_e$  and  $\nu_\mu$  system with the best-fit solar large mixing angle (LMA) parameters. Shown is the angle between each  $\mathbf{A}_p$  and  $\hat{\mathbf{z}}$ , which would determine evolution of each  $\mathbf{P}_p$  in the absence of the self-term. The actual angle between  $\mathbf{P}_p$  and  $\hat{\mathbf{z}}$  is shown in Fig. 2b, displaying the stunning synchronization of all momentum modes, to roughly the orientation of  $\mathbf{A}_p$  at the average momentum  $\langle p/T \rangle \simeq 3$ . Figure 3 shows the tiny magnitude of the angle between  $\mathbf{P}_p$  and  $\mathbf{I}$ , which is the result of the synchronization.

Now, we justify why taking the evolution of  $\mathbf{A}_{\text{eff}}$  to be effectively that of the average of  $\mathbf{A}_p$  luckily provides the nearly the correct evolution. For the case where collisional damping may be neglected and assuming that both synchronization and the close alignment of  $\mathbf{P}_p + \bar{\mathbf{P}}_p$  with  $\mathbf{I}$  holds, we may explicitly calculate  $\mathbf{A}_{\text{eff}}$  which describes the MSW-like transition (the expressions for  $\mathbf{A}_{\text{eff}}$  and  $p_{\text{sync}}$  were independently calculated in Ref. [27]). We

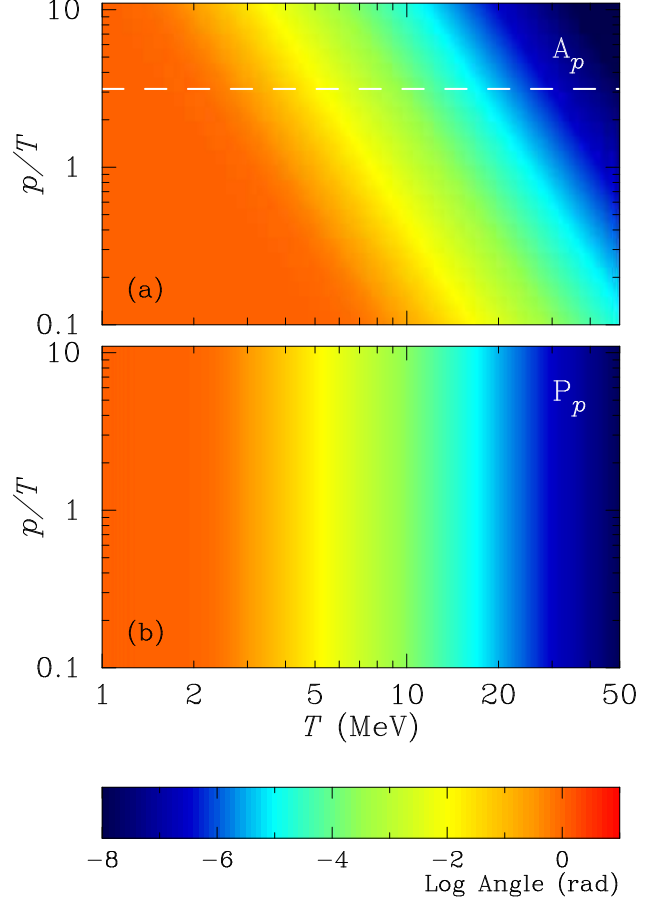


FIG. 2: The angle between  $\mathbf{A}_p$  and the  $z$  axis is shown in the upper panel, in color, as a function of the temperature of the universe (horizontally) and across the neutrino spectrum (vertically). In the lower panel, the angle between  $\mathbf{P}_p$  and the  $z$  axis is displayed in the same fashion. As detailed in the text, all  $\mathbf{P}_p$  ignore the momentum dependence of  $\mathbf{A}_p$  and are dramatically synchronized to a single effective momentum,  $p_{\text{sync}}/T \simeq \pi$ . That is, *all* of the  $\mathbf{P}_p$  follow the orientation (i.e., have the same color) of  $\mathbf{A}_p$  at  $p/T \simeq \pi$ , shown with a white horizontal dashed line.

find

$$\mathbf{A}_{\text{eff}} \simeq \xi \frac{\delta m_0^2}{2T} \left( \frac{3/2}{\pi^2 + \xi^2} \right) \left[ \sin 2\theta_0 \hat{\mathbf{x}} + (-\cos 2\theta_0 + Z) \hat{\mathbf{z}} \right], \quad (2.14)$$

where

$$Z = \frac{2T}{\delta m_0^2} \left( \frac{V^T}{p/T} \right) \left( \pi^2 + \frac{\xi^2}{2} \right). \quad (2.15)$$

Note that  $Z$  is negative so there is no resonance. It is helpful to reexpress Eq. (2.14) in terms of effective “synchronized” oscillation parameters as

$$\mathbf{A}_{\text{eff}} \equiv \Delta_{\text{sync}} (\sin 2\theta_{\text{sync}} \hat{\mathbf{x}} - \cos 2\theta_{\text{sync}} \hat{\mathbf{z}}), \quad (2.16)$$

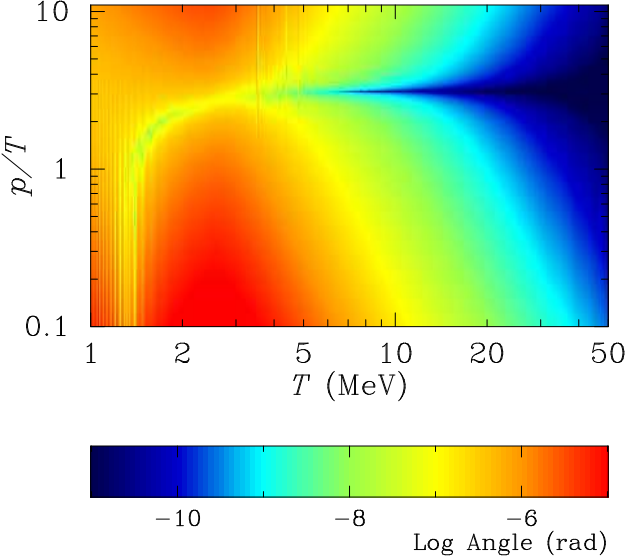


FIG. 3: We show the angle between individual  $\mathbf{P}_p$  and  $\mathbf{I}$  as a function of temperature of the universe (horizontally) and the neutrino spectrum (vertically). The angles are extremely small, indicating the degree of synchronization.

where the synchronized oscillation frequency is given by

$$\Delta_{\text{sync}} = \xi \frac{\delta m_0^2}{2T} \left( \frac{3/2}{\pi^2 + \xi^2} \right) \sqrt{\sin^2 2\theta_0 + (-\cos 2\theta_0 + Z)^2}. \quad (2.17)$$

The size of  $\Delta_{\text{sync}}$ , which is proportional to an overall factor of  $\xi$ , is not important in determining when the MSW-like transformation takes place.<sup>4</sup> It is the mixing angle  $\theta_{\text{sync}}$  that is important in describing the transformation resulting from the evolution into vacuum mass eigenstates. This angle (i.e., half of the angle between  $\mathbf{A}_{\text{eff}}$  with the  $z$  axis) is given by

$$\sin^2 2\theta_{\text{sync}} = \frac{\sin^2 2\theta_0}{\sin^2 2\theta_0 + (-\cos 2\theta_0 + Z)^2}, \quad (2.18)$$

and thus we find it is the mixing angle which would correspond to the momentum state

$$\frac{p_{\text{sync}}}{T} = \pi \sqrt{1 + \xi^2/2\pi^2} \simeq \pi. \quad (2.19)$$

This is one of our principal results, and indicates a remarkable coincidence. Namely, the apparently identical evolution for the synchronized system including the self-term and that found with a vanishing self-term only re-

sults from the fact that average momentum for a relativistic Fermi gas (with small chemical potential)

$$\langle p/T \rangle = \frac{7\pi^4}{180\zeta(3)} \simeq 3.15 \quad (2.20)$$

is approximately  $\pi$ , the effective momentum of the synchronized system (2.19) with  $\xi \ll \pi$ . One can observe in Fig. 2 that the effective mixing angle (the angle of  $\mathbf{A}_p$  with respect to the  $z$  axis) does in fact correspond to the way in which the state  $p/T \simeq 3$  would evolve in the absence of the self-term.

It is clear that  $\theta_{\text{sync}}$  depends only very weakly on the size of the initial asymmetry, and in particular the transformation will occur at almost the same temperature for any plausible initial  $\xi$ . Additionally, if  $\xi$  were very large, even a very small degree of flavor transformation would be sufficient to upset successful BBN. We have also numerically integrated the system for several initial asymmetries, and verified that the synchronized transformation is present for all asymmetries within the previous limit in Eq. (1.4).

Note that a large mixing angle is essential in obtaining flavor “equilibration,” i.e., that  $\xi_\mu^i$  is effectively transferred to  $\xi_e^f$  as shown by DHPPRS [19]. The underlying dynamics is simply the adiabatic evolution of the initial neutrinos into vacuum mass eigenstates. This would be exactly the usual MSW effect<sup>5</sup> if it were not for additional complexity of synchronization. We achieve equilibration in the sense that the initial asymmetry is partitioned across the flavors (with the ratio of the final  $\xi_e^f$  and  $\xi_{\mu,\tau}^f$  set by the vacuum mixing angle). This “equilibration” is simply a MSW transformation that leaves the ensemble in a coherent state. This is to be distinguished from equilibration in the conventional sense of a completely incoherent or relaxed state, i.e., one produced by collisions.

### III. NEUTRINO PROPERTIES AND ASYMMETRY TRANSFORMATION

Since the asymmetry in the electron neutrino number is the most stringently constrained, its enhancement due to coupling to the other flavors is crucial. The neutrino oscillation solution best fitting the observed solar electron neutrino flux and spectra is the region of mixing parameter space named the large mixing angle (LMA) solution, with maximum likelihood parameters for two-neutrino mixing of order  $\delta m_0^2 \approx 4 \times 10^{-5}$  eV<sup>2</sup> and  $\sin^2 2\theta_0 \approx 0.8$ . Since the LMA mixing is large but not maximal, the first mass state ( $|m_1\rangle$ ) is more closely associated with the elec-

<sup>4</sup> If  $V^T = 0$ , we find  $\Delta_{\text{sync}} \simeq \delta m_0^2/132T$  for  $\xi = 0.05$  in agreement with Ref. [19]. We note that the momentum scale  $p/T \simeq 132$  does not determine the character of the solution.

<sup>5</sup> Note, however, that for a normal hierarchy we do not have a resonance — the negative thermal potential makes the  $\nu_e$ ’s *lighter*, and does the same for  $\bar{\nu}_e$ .

tron neutrino and the other ( $|m_2\rangle$ ) less so, and in order to enable resonance in the sun,  $m_1 < m_2$ .

We also know from atmospheric neutrino observations that  $\mu$  and  $\tau$  neutrino flavors are maximally mixed superpositions (or nearly so) of two mass states  $|m_2\rangle$  and  $|m_3\rangle$ . Therefore, the flavor composition of mass state  $|m_2\rangle$  is that of a nearly maximal superposition, and complicates discussion of LMA mixing in neutrino environments where the flavor content of  $|m_2\rangle$  is of interest.

However, a powerful simplification can be made given maximally mixed (or more generally “similarly coupled”)  $\nu_\mu$  and  $\nu_\tau$ , which allows a linear transformation of the  $3 \times 3$  mixing matrix such that one effective flavor state  $|\nu_\tau^*\rangle$  is identically a vacuum mass eigenstate and decouples from the matter effects [28]. It is sufficient to follow the two remaining states  $|\nu_e\rangle$  and  $|\nu_\mu^*\rangle$ . This is only justified if the momentum state (or more exactly, momentum distributions) of the superimposed flavors  $|\nu_\mu\rangle$  and  $|\nu_\tau\rangle$  are indistinguishable. That is, the temperatures and chemical potentials of  $\nu_\mu$  and  $\nu_\tau$  should be equal, i.e.,  $\nu_\mu$ ,  $\nu_\tau$  should be equilibrated. The atmospheric neutrino results actually can provide that  $\nu_\mu$  and  $\nu_\tau$  are equilibrated, which we discuss in Section III B. Strictly speaking, the similar-coupling limit is exact only when  $U_{e3} = 0$ , and we consider the more general case below.

### A. Electron flavor transformation

Recall that we are interested in whether an asymmetry initially present in the poorly constrained  $\nu_\mu$  or  $\nu_\tau$  will convert into a stringently constrained  $\nu_e/\bar{\nu}_e$  asymmetry. We can analyze how the LMA mixing parameters evolve in the early universe through the effective two-neutrino system  $(\nu_e, \nu_\mu^*)$ . The initial system may be prepared by an unspecified leptogenesis mechanism to be in an unmixed state with the asymmetry in  $\nu_\mu^*$  ( $\xi_{\mu^*}^i \neq 0$ ) and no asymmetry in  $\nu_e$  ( $\xi_e^i = 0$ ) and remains in this state from damping by collisions. We have defined the direction  $+\hat{z}$  to correspond to the  $\nu_e$  flavor. Taking, for the sake of the example, the initial  $\xi_{\mu^*}^i$  to be negative, the vector  $\mathbf{I}$  will initially point in the  $+\hat{z}$  direction.

At initially high temperatures, the effective magnetic field vector  $\mathbf{A}_{\text{eff}}$  is dominated by the thermal lepton potential  $V^T$ , and is aligned in the  $-\hat{z}$  direction. As the universe cools,  $\mathbf{A}_{\text{eff}}$  rotates away from  $-\hat{z}$  and asymptotes to its vacuum value, which lies close to the  $+\hat{x}$  direction (i.e., the angle it makes with the  $z$  axis is  $2\theta_0$ ). A large vacuum mixing angle is clearly necessary for this MSW transformation to work.

For an initial asymmetry of  $|\xi_{\mu^*}^i| = 0.05$ , the evolution of the synchronized vector components  $J_i$  are shown in Fig. 4. The components are driven as a magnetic dipole adiabatically following the evolution of the magnetic field  $\mathbf{A}_{\text{eff}}$ . The evolution of  $P_i(\bar{P}_i)$  at the average momentum is the same if one excludes the self-potentials in Eq. (2.4). The power law growth of  $J_x$  is simply the evolution of the

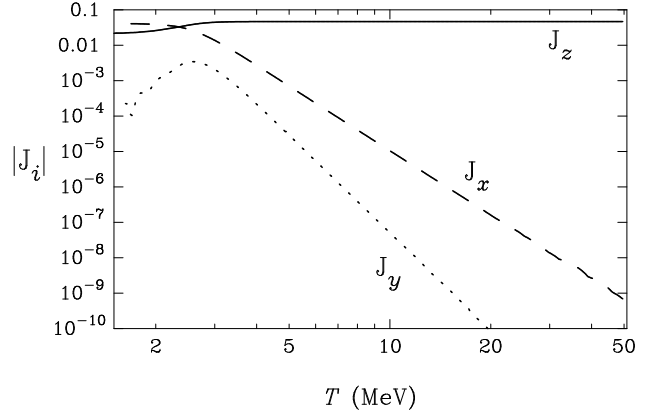


FIG. 4: The evolution of  $J_i$  in the synchronized case with LMA parameters. As described in the text, the behavior is essentially a MSW transformation  $\nu_e \leftrightarrow \nu_\mu^*$ . The antineutrinos  $|\bar{J}_i|$  evolve identically. The fact that  $J_y$  is never large demonstrates that all of the precession angles are small enough that the evolution is dominantly in the  $x - z$  plane. The evolution of  $P_i$  and  $\bar{P}_i$  at the average momentum is the same if one excludes the self-potentials in Eq. (2.4).

synchronized mixing angle

$$J_x \sim 2\theta_{\text{sync}} \sim \frac{1}{Z} \equiv \frac{\delta m_0^2 / 2p_{\text{sync}}}{V^T(p_{\text{sync}})} \sim T^{-6}, \quad (3.1)$$

and the growth of  $J_y \sim T^{-9}$  results directly from (2.11). Obviously, the transformation occurs when the orientation of  $\mathbf{J}$  rapidly evolves at  $\langle \Delta_p \rangle \sim \langle V^T \rangle$  at  $T \sim 2$  MeV. The temperature of the transition point in  $J_x$  scales only as  $(\delta m^2)^{1/6}$ , so the results are rather insensitive to the uncertainty in the LMA  $\delta m^2$ . The antineutrinos evolve identically by following the vector  $-\mathbf{A}_{\text{eff}}$ . The final state of the asymmetry after the MSW transformation entering the nucleosynthesis epoch is then transferred in proportion to the vacuum mixing amplitude between the two flavors, i.e.,  $J_z(1 \text{ MeV})$ :

$$\xi_e^f = \left( \frac{1 - \cos 2\theta_0}{2} \right) \xi_{\mu^*}^i, \quad (3.2)$$

$$\xi_{\mu^*}^f = \left( \frac{1 + \cos 2\theta_0}{2} \right) \xi_{\mu^*}^i. \quad (3.3)$$

(Some care must be taken in interpreting the limits on  $\xi^f$ , since the final distributions are not exactly thermal, as they are superpositions of Fermi-Dirac distributions with different chemical potentials.) Obviously, complete “equilibration” or  $\xi_e^f = \xi_{\mu^*}^f$  only occurs for maximal mixing. The antineutrino chemical potential evolves to the values  $\bar{\xi}_e^f = -\xi_e^f$  and  $\bar{\xi}_{\mu^*}^f = -\xi_{\mu^*}^f$ . We note that collisions (which we have neglected) will help make the flavor transformation more complete and thus should reduce the sensitivity to the mixing angle.

## B. Mu-tau flavor transformation

Maximal neutrino mixing as indicated by the Super-Kamiokande observations of atmospheric neutrinos has nearly identical implications for the evolution of asymmetries between  $\nu_\mu$  and  $\nu_\tau$ . Because of the hierarchy  $\delta m_{\text{atm}}^2 \gg \delta m_{\text{LMA}}^2$ ,  $\langle \Delta_p \rangle \sim \langle V^T \rangle$  at the higher temperature  $T \sim 10$  MeV. Necessary in driving the flavor evolution here is the presence of the remnant thermally produced charged muons with energy density

$$\rho_{\mu^\pm} = \frac{1}{\pi^2} \int p^2 dp \frac{\sqrt{p^2 + m_\mu^2}}{1 + \exp(\sqrt{p^2 + m_\mu^2}/T)}. \quad (3.4)$$

Though far from the thermal abundance of  $e^\pm$  at  $T \sim 20$  MeV, real muons remain enough to dictate the flavor evolution. However, since  $T < m_\mu$ , the thermal potential from Eq. (2.8) is modified as  $\langle E_{\mu^\pm} \rangle \rightarrow \frac{3}{4} \langle E_{\mu^\pm} + p^2/3E_{\mu^\pm} \rangle$  [29]. We solved the evolution of this case numerically, explicitly including the thermal abundance of  $\mu^\pm$ , whose disappearance accelerates the growth of  $J_x$  and  $J_y$  away from the power-law growth in the previous LMA case, but for simplicity have ignored collisions (Fig. 5). Maximal mixing then gives an equilibration  $\xi_\mu^f = \xi_\tau^f$ , which allows the application of the simplifying basis transformation of the previous section. Inclusion of collisions would damp the oscillations at low temperatures but not the transformation, as found by DHPPRS [19].

Interestingly, in the case of evolution without the presence of thermal  $\mu^\pm$ , the evolution is different, with pure synchronized vacuum oscillations taking place (rotation in the  $z - y$  plane) after the Hubble time exceeds the oscillation time. Collisions, which we have omitted, would modify the oscillations seen here.

## C. Effects of $U_{e3}$

The possibility of a nonzero value of  $U_{e3}$  obstructs the simplifying linear transformation to the basis  $|\nu_e\rangle$  and  $|\nu_\mu^*\rangle$ . However, nonzero  $U_{e3}$  may allow partial equilibration of  $\xi_\mu, \xi_\tau$  into  $\xi_e$  earlier, at  $T \sim 5$  MeV. For solar LMA mixing, significant transformation will always occur at  $T \sim 2$  MeV so the value of  $U_{e3}$  will not alter the basic outcome. However, substantial equilibration at 5 MeV (well before the beta-equilibrium freeze-out) makes the general conclusions even more inevitable.

There are, however, some subtleties associated with the sign of  $\delta m_{\text{atm}}^2$  — that is, whether the neutrino spectrum has a normal or inverted hierarchy.<sup>6</sup> For a normal

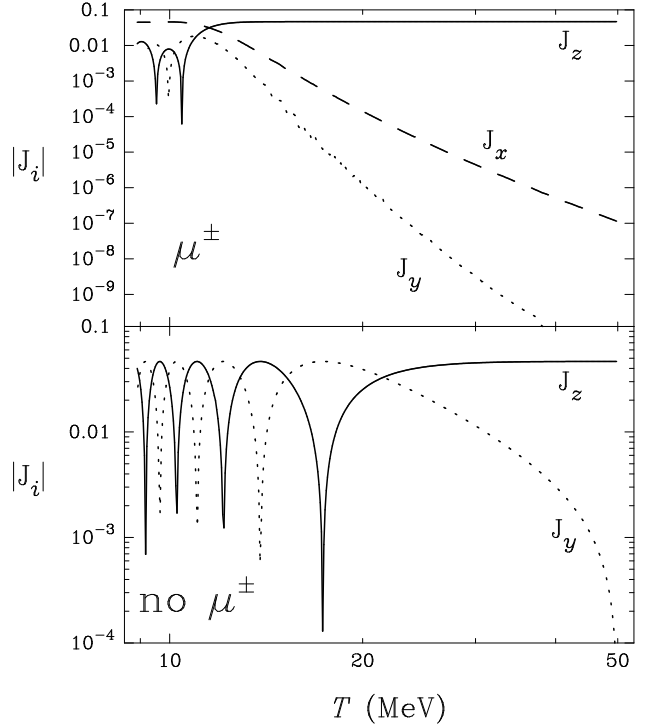


FIG. 5: The evolution of  $J_i$  ( $\bar{J}_i$  are identical) for the mu and tau neutrino transformation with and without the inclusion of thermal  $\mu^\pm$  pairs. The spiky features indicate real oscillations going through zero, and the depth of the spikes on the logarithmic scale is an artifact of numerical sampling. Those oscillations are real and are determined by the atmospheric  $\delta m_0^2$ . In the lower panel,  $J_x$  is zero since the mixing angle is maximal. Collisions have been ignored.

hierarchy, the fact the thermal potential makes the  $\nu_e$ 's (and  $\bar{\nu}_e$ 's) lighter implies that that no resonance conditions can be satisfied in the early universe. With an inverted hierarchy, however, a  $\nu_e - \nu_\mu^*$  resonance will occur when  $V^T \sim \delta m_{\text{atm}}^2$ . We plot in Fig. 6 level crossing diagrams for neutrinos of the average energy in the absence of the self potential. As discussed above, this is a very good description of the evolution of the entire neutrino distribution.

The  $U_{e3}$  mixing angle is constrained to be small [30], and as such, coherent evolution will not lead to large flavor transformation (for the inverted hierarchy, coherent evolution through the resonance would swap asymmetries between flavors). However, at  $T \sim 5$  MeV collisional processes are still highly important and will help achieve equilibration. This should be somewhat more effective for the inverted case (where the mixing angle goes through a maximum) as collisions equilibrate most effectively when mixing angles are large.

<sup>6</sup> The sign of the solar  $\delta m^2$  is determined by the requirement that there be a MSW transition in the Sun, which precludes a resonance in the early universe (for both neutrinos and antineutrinos). There is, however, no such constraint of the sign of the atmospheric  $\delta m^2$ .

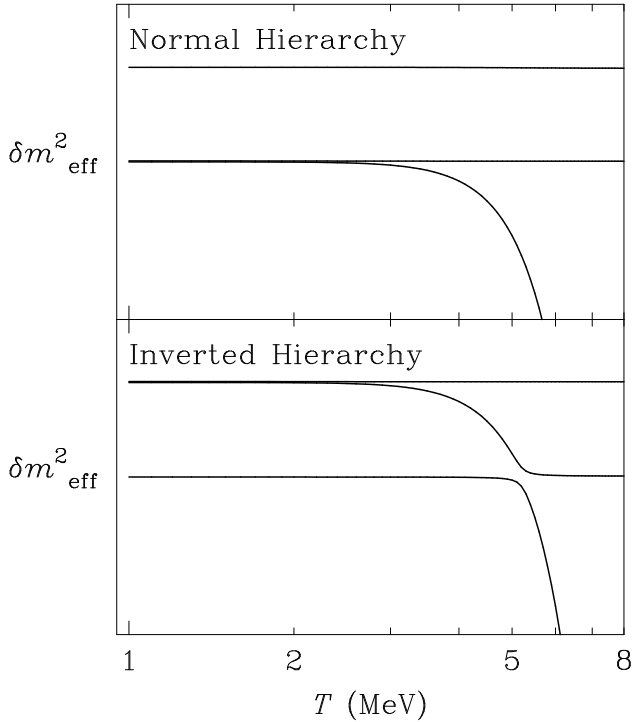


FIG. 6: Level-crossing diagrams for neutrinos of the average momentum in the absence of the self-potential. In the upper panel we have a normal hierarchy, where the neutrino mass eigenstates asymptote to their vacuum values, without ever going through a resonance. This is to be contrasted with the inverted hierarchy shown in the lower panel where nonzero  $U_{e3}$  leads to a resonance at  $T \sim 5$  MeV.

#### IV. NEW CONSTRAINTS

The electron neutrino asymmetry  $\xi_e$  is limited by its effects on the primordial  ${}^4\text{He}$  abundance,  $Y_p$ . At nucleosynthesis, nearly all neutrons are incorporated into  ${}^4\text{He}$  nuclei, and  $Y_p$  production is limited by the neutron fraction, set by the freeze-out of beta equilibrium at  $T \simeq 1$  MeV. The change in the neutron to proton ratio with non-zero  $\xi_e$  is simply a Boltzmann factor  $n/p \propto e^{-\xi_e} \approx 1 - \xi_e$ . And since  $Y_p \propto n/p$ , the uncertainty in the constraint on  $\xi_e$  is directly related to the uncertainty in the primordial helium abundance  $\Delta Y_p$ ,

$$\Delta\xi_e \approx \frac{\Delta Y_p}{Y_p}. \quad (4.1)$$

Therefore, one can be very conservative regarding the error on the primordial abundance, e.g.,  $\Delta Y_p \approx \pm 0.010$  [31] and still limit  $\Delta\xi_e \approx \pm 0.04$ , or equivalently,  $|L_e| \lesssim 0.03$ . This method ultimately relies on the uncertainty (mostly systematic) in the primordial abundance of  ${}^4\text{He}$ . Refinement of this constraint may be possible by applying CMB priors to BBN predictions combined with reduced systematic uncertainties of observed primordial element abundances [32].

Analysis of synchronized transformation of neutrino asymmetries indirectly translates the constraints on  $\xi_e^f$  to  $\xi_\mu^i$  and  $\xi_\tau^i$ . In the extreme scenario, an asymmetry  $\xi_{\mu,\tau}^i$  in  $\nu_\mu$  ( $\nu_\tau$ ) is equilibrated with  $\nu_\tau$  ( $\nu_\mu$ ) for maximal mixing, such that the state  $\nu_\mu^*$  has  $\xi_{\mu^*} = 0.5\xi_{\mu,\tau}^i$ . The LMA solution transforms  $\xi_{\mu^*}$  as Eq. (3.3) so that

$$\xi_e^f = \left( \frac{1 - \cos 2\theta_0}{4} \right) \xi_{\mu,\tau}^i. \quad (4.2)$$

For the best-fit LMA mixing angle  $\sin^2 2\theta_0 \approx 0.8$ , the limit on an initial asymmetry is  $\xi_{\mu,\tau}^i \lesssim 0.3$ . However, the LMA mixing angle is not precisely specified. The lower end of the 95% confidence level (C.L.) region has  $\sin^2 2\theta_0 \approx 0.6$ , for which the limit on the initial asymmetry is considerably weaker<sup>7</sup>  $\xi_{\mu,\tau}^i \lesssim 0.5$ . The effective “2 $\sigma$ ” limit therefore is actually an order of magnitude larger than that given in DHPPRS since a “small-angle” LMA solution reduces the transformation amplitude considerably. The sensitivity of the KamLAND experiment to the LMA parameter space can confirm the LMA parameters [33] and potentially reduce the mixing angle uncertainty, and thus improve constraints on the lepton number.

#### V. DISCUSSION AND CONCLUSIONS

Due to synchronization by the neutrino self-potential, transformation of a large fraction of any asymmetries in  $\nu_\mu$  or  $\nu_\tau$  number to  $\nu_e$  is an inescapable consequence of the near bimaximal mixing framework emerging for the neutrino mass matrix. We have performed a full numerical integration of the evolution equations in Eq. (2.4). The numerical solution is nontrivial due to stiff, nonlinear equations with terms whose time scales vary by several orders of magnitude. We confirm the numerical results of DHPPRS, and agree that large initial asymmetries in  $\nu_\mu$  and  $\nu_\tau$  are effectively transformed into a  $\nu_e$  asymmetry, so that the bound from BBN bounds all [19].

In addition, we have shown numerically that the coupled evolution of the full-momentum results can also be obtained in the average-momentum case when the nonlinear coupling is neglected. The transfer of neutrino asymmetries between flavors occurs identically even when ignoring the numerically dominant self-potential. In Eq. (2.19) we have derived that the self-potential drives a synchronization of all momenta to a momentum mode  $p/T = \pi$ , so that the system by numerical coincidence closely follows the average momentum case  $p/T \simeq 3.15$ .

We conclude by considering the following implications of these results:

---

<sup>7</sup> Note that we expect this limit would be tighter were we to include the effect of collisions.

(1) The uncertainty in the lepton number of the universe may be reduced by up to two orders of magnitude. However, the most conservative limits place

$$|\xi_e^f| \lesssim 0.04, \quad (5.1)$$

$$|\xi_\mu^i + \xi_\tau^i| \lesssim 0.5, \quad (5.2)$$

( $|L_e| \lesssim 0.03$  and  $|L_\mu + L_\tau| < 0.4$ ). These limits will be improved by reducing systematic uncertainties in the inferred primordial  ${}^4\text{He}$  abundance and the precise determination of the baryon density by satellite anisotropy experiments Microwave Anisotropy Probe (MAP) and Planck [34]. It also may be improved by verification of the LMA parameters by KamLAND, particularly if the mixing angle is at the large end of the presently allowed range. The upcoming data from SNO [35] will also play a very important role in reducing the mixing parameter uncertainties.

(2) Because effectively asymmetries in any neutrino flavor will affect beta equilibrium, the stringent limits (5.1) consequentially eliminate the possibility of degenerate BBN [20], since an increase the expansion rate with large  $|\xi_{\mu,\tau}| \sim 1$  can no longer be compensated by a small  $\xi_e \sim 0.1$ .

(3) The above limits on degeneracy in terms of extra relativistic degrees of freedom  $\Delta N_\nu$  [see Eq. (1.3)] are impressively small:  $\Delta N_\nu \lesssim 0.004$  for the best-fit LMA solution, and  $\Delta N_\nu \lesssim 0.2$  for the lower limit on the mixing angle in the LMA solution. DHPPRS suggest that  $\Delta N_\nu$  can be eliminated as a cosmological parameter in upcoming fits to the precision CMB data [8]. It is certainly true that  $\xi$  can be eliminated, but that is not the only possible contribution to  $\Delta N_\nu$ . *If any nonstandard contribution to the relativistic energy density were to be detected via the CMB, its origin would be something more exotic than degenerate neutrinos*, e.g., the decay of a massive particle to relativistic species after BBN but before CMB decoupling [36].

(4) It is actually still possible that the upper limit for

$\xi_e$  in Eq. (1.4) be fulfilled. Strictly speaking, we have set tight new degeneracy limits assuming no non-standard contribution to the energy density at the time of BBN. It is conceivable that  $\xi_e \sim \xi_\mu \sim \xi_\tau \sim 0.2$  if another relativistic particle or scalar field contributes the extra energy density required to compensate for the large  $\nu_e$  chemical potential. In this case, flavor-transformation improves the current  $\xi_{\mu,\tau}$  limits by at most an order of magnitude. Such an unnatural scenario can be detected by comparison with the CMB.

(5) A possible complication to the scenario presented here could be mixing with a light sterile neutrino. Obviously, if the LSND result is confirmed by MiniBooNE, then the physics will be much more complicated than assumed here. If the LSND result is not confirmed, there is still the possibility of subdominant mixing to steriles that may be difficult to detect in neutrino oscillation experiments, but which may still play an important role in the early universe. Such scenarios have not yet been explored.

(6) A final complication is the yet-unexcluded possibility of a low reheating temperature ( $T \sim 1$  MeV) [37], such that the initial conditions of thermal or chemical equilibrium for neutrinos for the analysis presented here is invalid. Stronger constraints on low-temperature reheating scenarios may be obtained by studying their effects on the light element abundances in detail.

## Acknowledgments

We thank Scott Dodelson, George Fuller, Ray Sawyer, Ray Volkas, and Yvonne Wong for useful discussions. K.N.A., J.F.B., and N.F.B. were supported by Fermilab, which is operated by URA under DOE contract No. DE-AC02-76CH03000, and were additionally supported by NASA under NAG5-10842.

- 
- [1] D. N. Schramm and M. S. Turner, Rev. Mod. Phys. **70**, 303 (1998).
  - [2] C. Pryke, N. W. Halverson, E. M. Leitch, J. Kovac, J. E. Carlstrom, W. L. Holzapfel, and M. Dragovan, Astrophys. J. **568** (2002) 46; P. de Bernardis *et al.*, *ibid.* **564** (2002) 559.
  - [3] M. S. Turner, astro-ph/0106035.
  - [4] W. J. Percival *et al.*, Mon. Not. R. Astron. Soc. **327**, 1297 (2001).
  - [5] I. Affleck and M. Dine, Nucl. Phys. **B249**, 361 (1985); A. Casas, W. Y. Cheng, and G. Gelmini, *ibid.* 297 (1999).
  - [6] R. Foot, M. J. Thomson, and R. R. Volkas, Phys. Rev. D **53**, 5349 (1996).
  - [7] S. Hannestad, Phys. Rev. Lett. **85**, 4203 (2000).
  - [8] W. H. Kinney and A. Riotto, Phys. Rev. Lett. **83**, 3366 (1999); R. E. Lopez, S. Dodelson, A. Heckler, and M. S. Turner, *ibid.* **82**, 3952 (1999).
  - [9] S. H. Hansen, G. Mangano, A. Melchiorri, G. Miele, and O. Pisanti, Phys. Rev. D **65**, 023511 (2002).
  - [10] J. P. Kneller, R. J. Scherrer, G. Steigman and T. P. Walker, Phys. Rev. D **64**, 123506 (2001).
  - [11] Homestake Collaboration, B. T. Cleveland *et al.*, Astrophys. J. **496**, 505 (1998); GALLEX Collaboration, W. Hampel *et al.*, Phys. Lett. B **447**, 127 (1999); SAGE Collaboration, J. N. Abdurashitov *et al.*, Phys. Rev. C **60**, 055801 (1999); Super-Kamiokande Collaboration, S. Fukuda *et al.*, Phys. Rev. Lett. **86**, 5651 (2001); 5656 (2001); GNO Collaboration, M. Altmann *et al.*, Phys. Lett. B **490**, 16 (2000); SNO Collaboration, Q. R. Ahmad *et al.*, Phys. Rev. Lett. **87**, 071301 (2001).

- [12] Super-Kamiokande Collaboration, S. Fukuda *et al.*, Phys. Rev. Lett. **85**, 3999 (2000);  
Super-Kamiokande Collaboration, Y. Fukuda *et al.*, *ibid.* **81**, 1562 (1998).
- [13] LSND Collaboration, A. Aguilar *et al.*, Phys. Rev. D **64**, 112007 (2001).
- [14] M. C. Gonzalez-Garcia and Y. Nir, hep-ph/0202058;  
C. Giunti, J. High Energy Phys. **0001**, 032 (2000).
- [15] P. Di Bari, Phys. Rev. D **65**, 043509 (2002);  
N. F. Bell, R. Foot, and R. R. Volkas, *ibid.* **58**, 105010 (1998);  
K. Abazajian, G. M. Fuller, and X. Shi, *ibid.* **62**, 093003 (2000).
- [16] MiniBooNE Collaboration, A. Bazarko, Nucl. Phys. B (Proc. Suppl.) **91**, 210 (2000).
- [17] C. Lunardini and A. Y. Smirnov, Phys. Rev. D **64**, 073006 (2001).
- [18] M. J. Savage, R. A. Malaney and G. M. Fuller, Astrophys. J. **368**, 1 (1991).
- [19] (DHPPRS): A. D. Dolgov, S. H. Hansen, S. Pastor, S. T. Petcov, G. G. Raffelt, and D. V. Semikoz, Nucl. Phys. **B632**, 363 (2002).
- [20] H. S. Kang and G. Steigman, Nucl. Phys. **B372**, 494 (1992);  
S. Esposito, G. Mangano, G. Miele, and O. Pisanti, J. High Energy Phys. **0009**, 038 (2000);  
M. Orito, T. Kajino, G. J. Mathews and Y. Wang, Phys. Rev. D **65**, 123504 (2002).
- [21] L. Stodolsky, Phys. Rev. D **36**, 2273 (1987);  
B. H. McKellar and M. J. Thomson, *ibid.* **49**, 2710 (1994).
- [22] J. Pantaleone, Phys. Lett. B **287**, 128 (1992).
- [23] S. Pastor, G. G. Raffelt, and D. V. Semikoz, Phys. Rev. D **65**, 053011 (2002).
- [24] N. F. Bell, R. F. Sawyer, and R. R. Volkas, Phys. Lett. B **500**, 16 (2001).
- [25] S. Samuel, Phys. Rev. D **48**, 1462 (1993);  
V. A. Kostelecky and S. Samuel, *ibid.* **52**, 621 (1995);  
S. Samuel, *ibid.* **53**, 5382 (1996);  
J. Pantaleone, *ibid.* **58**, 073002 (1998).
- [26] G. Sigl and G. Raffelt, Nucl. Phys. B **406**, 423 (1993).
- [27] Y. Y. Y. Wong, Phys. Rev. D (to be published), hep-ph/0203180.
- [28] D. O. Caldwell, G. M. Fuller, and Y. Z. Qian, Phys. Rev. D **61**, 123005 (2000);  
A. B. Balantekin and G. M. Fuller, Phys. Lett. B **471**, 195 (1999).
- [29] D. Notzold and G. Raffelt, Nucl. Phys. **B307**, 924 (1988);  
J. C. D'Olivo, J. F. Nieves and M. Torres, Phys. Rev. D **46**, 1172 (1992).
- [30] CHOOZ Collaboration, M. Apollonio *et al.*, Phys. Lett. B **466**, 415 (1999);  
Palo Verde Collaboration, F. Boehm *et al.*, Phys. Rev. D **64**, 112001 (2001).
- [31] K. A. Olive and E. Skillman, New Astron. **6**, 246 (2001).
- [32] R. H. Cyburt, B. D. Fields, and K. A. Olive, Astropart. Phys. **17**, 87 (2002).
- [33] KamLAND Collaboration, A. Piepke, Nucl. Phys. B (Proc. Suppl.) **91**, 99 (2001).
- [34] W. Hu and S. Dodelson, astro-ph/0110414.
- [35] SNO Collaboration, J. R. Klein, hep-ex/0111040.
- [36] S. Hannestad, Phys. Rev. D **64**, 083002 (2001).
- [37] M. Kawasaki, K. Kohri, and N. Sugiyama, Phys. Rev. Lett. **82**, 4168 (1999);  
G. F. Giudice, E. W. Kolb, and A. Riotto, Phys. Rev. D **64**, 023508 (2001).